CHAPTER 5

PARAMETRIC ANALYSIS OF THE RVEHS

This chapter presents a parametric analysis of the proposed parabolic and exponentially tapering width RVEH. The first part discusses the effects of parabolic taper parameter, piezoelectric patch to host beam thickness ratio, harvester's length, and the overall radius of rotation on the RVEH's OC voltage responses and VPM. The second part presents the effects of these parameters on the exponentially tapering RVEH's frequency responses along with the OC voltage and VPM. Finally, a strategy is proposed to select the optimum configuration parameters for any driving frequency to achieve frequency matching.

5.1 Parametric Analysis of the Parabolic Tapering RVEH

The parametric analysis of the RVEH is conducted for four performance influencing parameters; taper parameter, the thickness ratio, piezoelectric coupled beam length, and overall radius of rotation.

5.1.1 Taper parameter study

The peak OC voltage response of the RVEH against the input driving frequency for a set of five different taper parameter values (0, 0.2, 0.4, 0.6, and 0.5) is depicted in Figure 5.1. The other parameters (t_p =0.254 mm, l =72 mm, b_0 =50 mm, t_h =0.5 mm, r =7.5 mm) are constant. It can be observed that the output voltage from the harvester decreases with an increase in the taper parameter. This is obviously due to the availability of less piezoelectric surface area with higher taper parameter values. At 12.2 Hz driving frequency, the generated voltage is decreased from 565.4063mV to 466.1106 mV when the taper parameter is increased from 0 to 0.8.

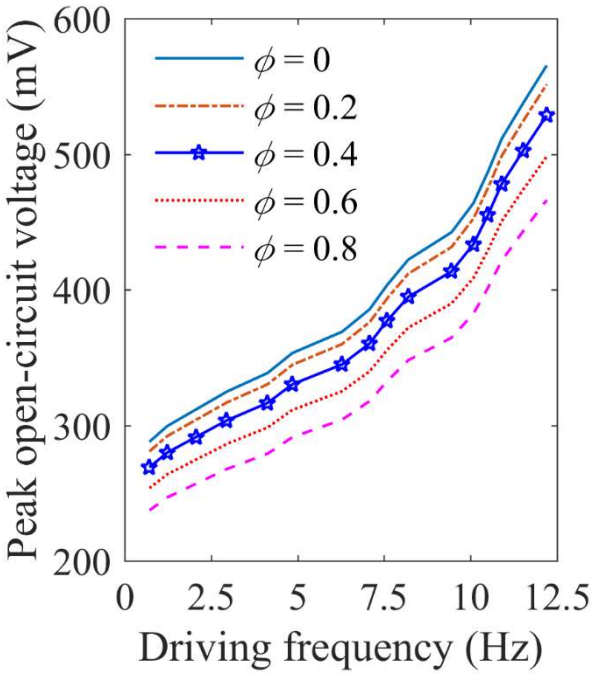

Figure 5.1 Effect of the variation of taper parameter on the RVEH's response, the peak open-circuit voltage against driving frequency

Since the mass of the harvester is also reduced with an increase in the taper parameter, the VPM of the harvester will not essentially follow the trend of the peak generated voltage against the taper parameter. Therefore, the VPM of the harvester is considered as the performance evaluation criteria of the harvester. The VPM of the harvester against the driving frequencies for the five ϕ values are shown in Figure 5.2. It can be observed that the VPM of the system with $\phi = 0$ is the lowest, and $\phi = 0.8$ is the highest. At 12.2 Hz driving frequency, the VPM is increased from 15.48V/Kg to 19.40 V/Kg when the taper parameter is increased from 0 to 0.8. Even though a high taper parameter system produces the highest VPM, the peak output voltage limits the use of high taper parameters.

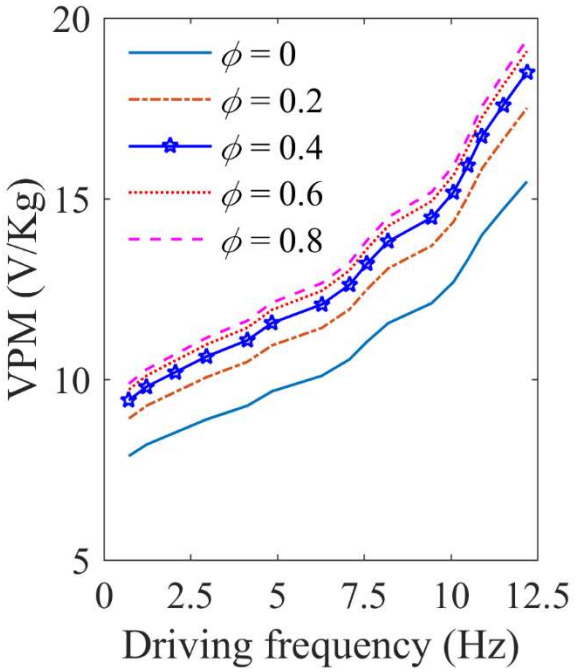

Figure 5.2 The VPM of the RVEH against the driving frequency for taper parameters 0 – 0.8

5.1.2 Thickness ratio study

In this part, the effects of the thickness ratio on the RVEH's open-circuit responses are studied. The thickness ratio is varied by changing the host beam thickness and keeping the patch thickness constant. Figure 5.3 displays the peak OC output voltage of the RVEH for five different (0.847, 0.635, 0.508, 0.423, and 0.363) values of the thickness ratios. The other parameters considered are t_p =0.254 mm, l =72 mm, ϕ =0.4, b_0 =50 mm, and l' =7.5 mm.

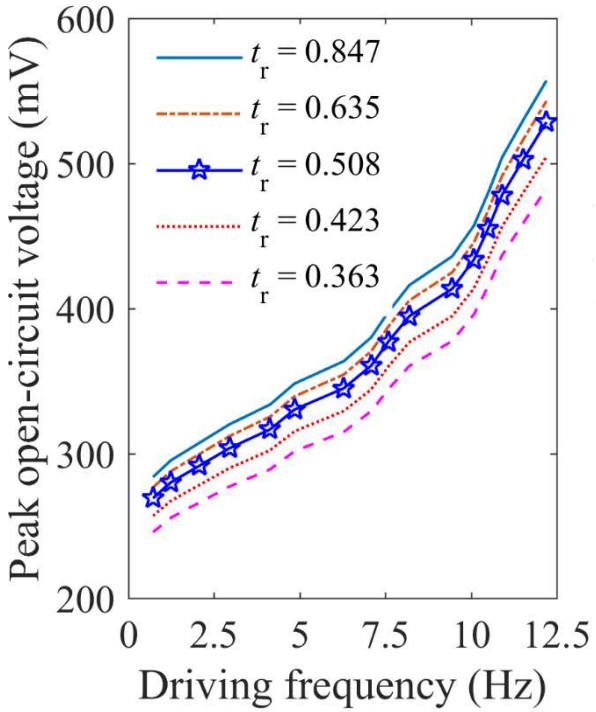

Figure 5.3 Effect of the variation of thickness ratio on the RVEH's response; the peak open-circuit voltage against driving frequency

It can be noticed that the OC voltage response of the harvester is increased with an increase in the thickness ratio. The flexural stiffness of the system is decreased as the thickness of the host beam is reduced, which in turn increases the amplitude of vibration

of the structure. Because of those higher amplitudes, the system's voltage responses are increased. At 12.2 Hz driving frequency, the generated voltage increases from 482.4703 to 557.1087 mV when the thickness ratio is increased from 0.363 to 0.847.

The VPM of the harvester against the driving frequencies for the five t_r values are displayed in Figure 5.4. It can be noticed that the VPM of the system with t_r =0.363 is the lowest, and t_r =0.847 is the highest. At 12.2 Hz driving frequency, the VPM increases from 16.256V/Kg to 20.297 V/Kg when the thickness ratio increases from 0.363 to 0.847. Although a system with a thinner host beam produces the highest VPM, the system's overall stability sets the limit on the use of high thickness ratios. The stability of the system decreases with a reduction in flexural rigidity.

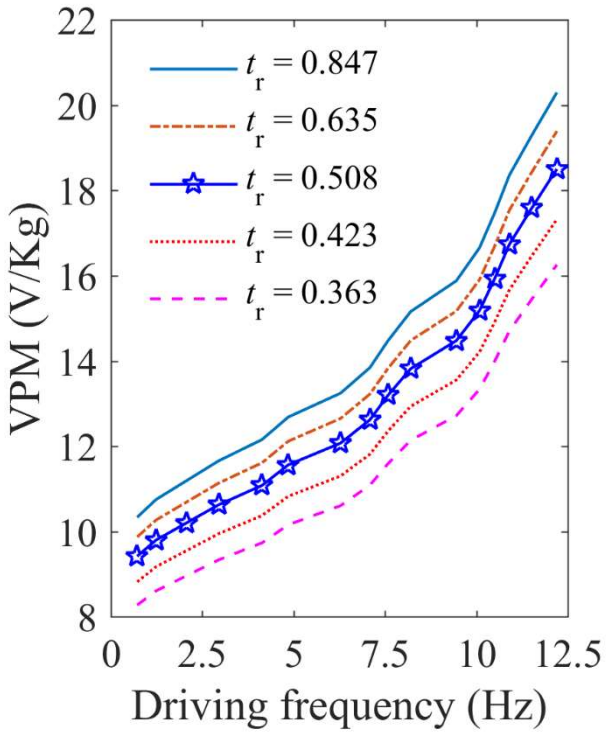

Figure 5.4 The VPM against the driving frequency for thickness ratios 0.363 – 0.847

5.1.3 Length of piezoelectric coupled beam study

Figure 5.5 displays the harvester's open-circuit voltage curves for various piezoelectric beam lengths (l = 52, 62, 72, 82, and 92 mm) and driving frequencies with t_p = 0.254 mm, ϕ = 0.4, b_0 = 50 mm, t_h = 0.5 mm, r = 7.5 mm. The generated voltage increased significantly with an increase in the active length. This is because of the availability of more piezoelectric material. At 12.2 Hz driving frequency, the generated voltage increases from 401.7368 mV to 607.7339 mV when the beam length increases from 52 mm to 92 mm.

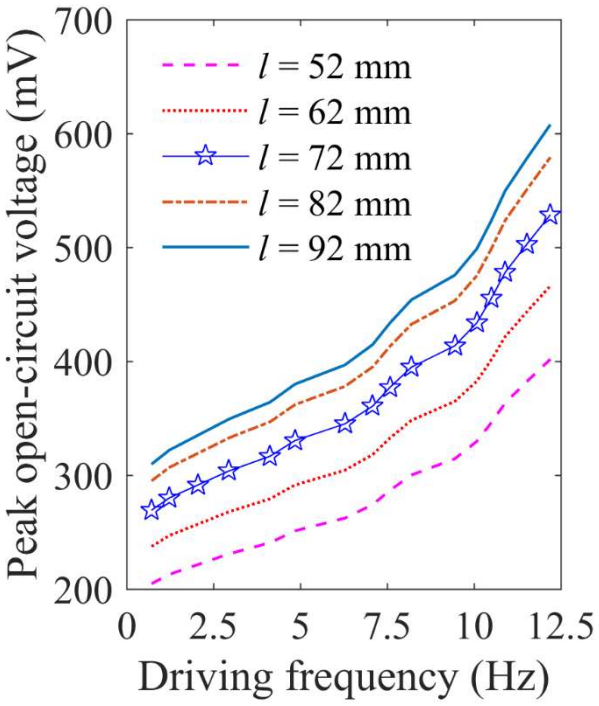

Figure 5.5 Effect of the variation of piezoelectric coupled beam length on the RVEH's response; the peak OC voltage against driving frequency

The VPM of the harvester against the driving frequencies for the five *l* values is given in Figure 5.6. It can be noticed that the VPM of the system with *l* = 52 mm is the lowest,

and l = 92 mm is the highest. At 12.2 Hz driving frequency, the VPM is increased from 16.606 V/Kg to 19.525 V/Kg when l is increased from 52mm to 92 mm. Although raising the active length enhances the RVEH's generated voltage, the harvester's overall size imposes restrictions on the harvester's length.

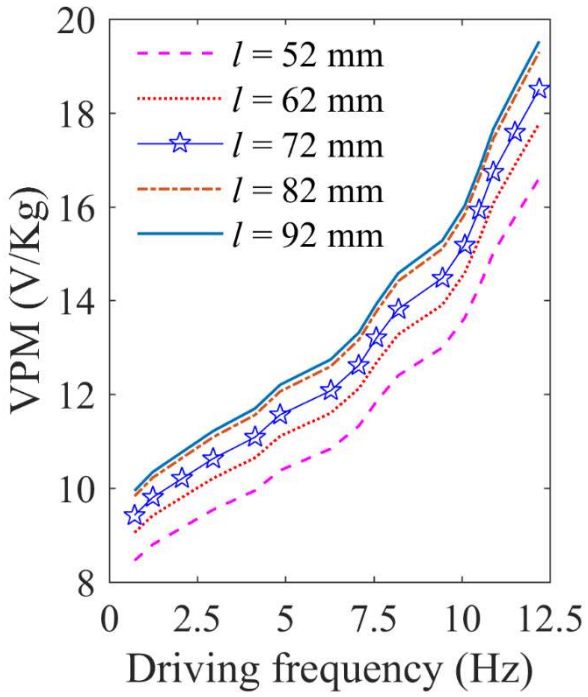

Figure 5.6 The VPM against the driving frequency for lengths 52 – 92 mm

5.1.4 Overall radius of rotation study

The effects of the overall radius of rotation on the RVEH's open-circuit responses are studied in this section. The r_o is varied by changing r and treating l as constant. Figure 5.7 displays the peak open-circuit output voltage of the RVEH for five different (77, 79.5, 82, 84.5, and 87 mm) values of r_o. The other parameters considered are t_p = 0.254

mm, $l = 72$ mm, $\phi = 0.4$, $b_0 = 50$ mm, and $t_h = 0.5$ mm. It can be noticed that the open-circuit response of the harvester is decreased with an increase in the overall radius of rotation. An increase in r_o, shifts the mass centre of the system away from the axis of rotation, consequentially increasing the centrifugal force in the system. The resultant centrifugal force tends to stabilize the system; as a result, the system's voltage responses are decreased. At 12.2 Hz driving frequency, the generated voltage is dropped from 559.8873 mV to 420.6079 mV when the r_o is increased from 77 mm to 87 mm.

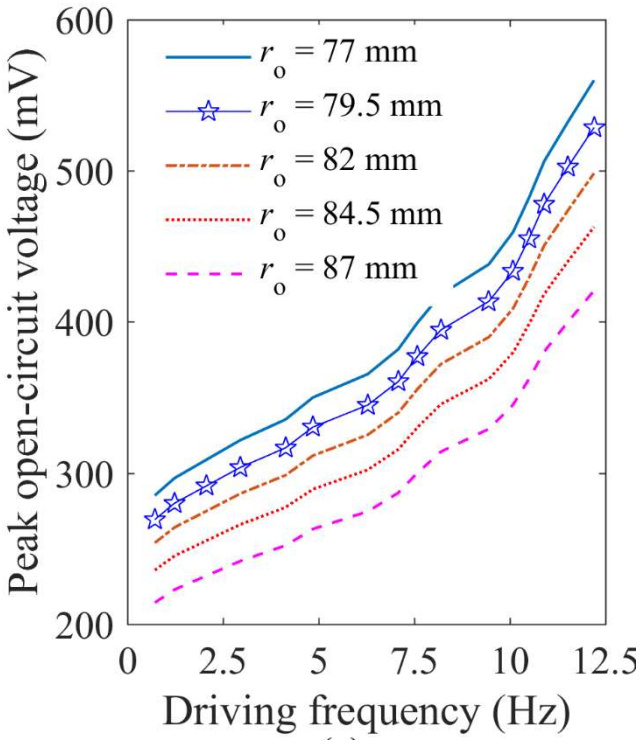

Figure 5.7 Effect of the variation of overall radius of rotation on the RVEH's response; the peak OC voltage against driving frequency

The VPM of the harvester against the driving frequencies for the five r_o values are given in Figure 5.8. It can be noticed that the VPM of the system with $r_o = 87$ mm is the

lowest, and r_o = 77 mm is the highest. At 12.2 Hz driving frequency, the VPM is decreased from 19.6018 V/Kg to 14.7256 V/Kg when the r_o is increased from 77 mm to 87 mm. Although a system with the lowest r_o produces the highest VPM, the diameter of the rotating shaft limits the use of a low overall radius of rotation.

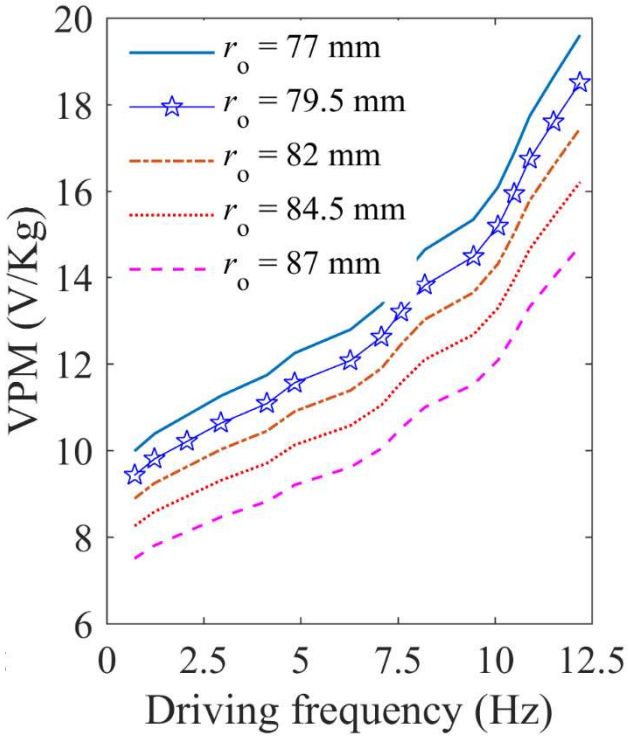

Figure 5.8 The VPM against the driving frequency for overall radiuses 77 – 87 mm

Vibration energy harvesters are generally modelled to operate at a fixed driving frequency(Chand and Tyagi, 2021; Wang et al., 2020). Therefore, the harvester's calculated VPM (CV) for different ϕ, t_r, l, and r_o values for a particular operating frequency (12 Hz) are presented in Figures 5.1b to 5.4b are shown in Figures 5.9a to 5.9d. The fitting curves (FC) for all the cases are also obtained and presented. The

fitting curves can be used to determine the harvester's VPM for a given parameter value.

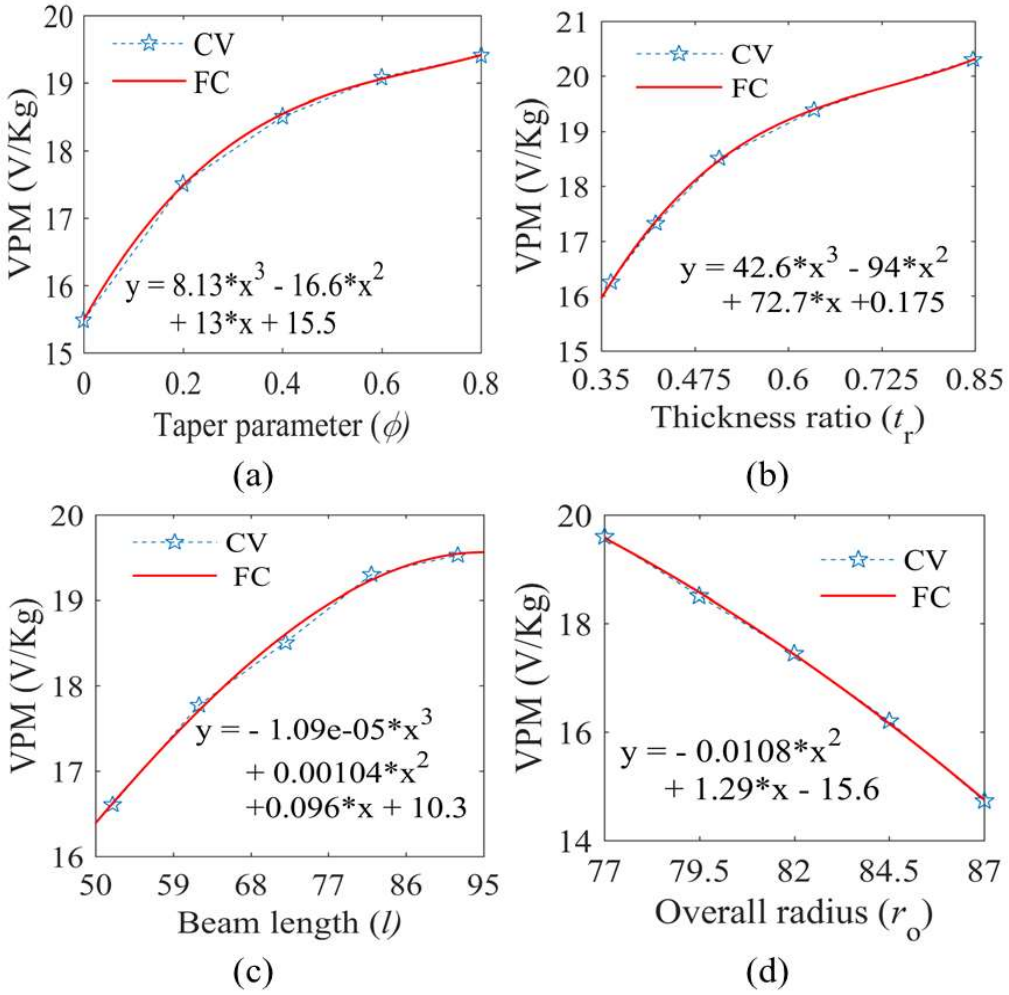

Figure 5.9 The calculated VPM of the harvester and the respective fitting curves against (a) ϕ, (b) t_r, (c) l, and (d) r_o

5.2 Parametric Analysis of Exponentially Tapering RVEH

In this case, two types of parameters that affect the harvester's performance are identified. The first category is operational in manipulating the fundamental frequency for energy harvesting, where zero-driving-frequency variation governs. The second category is responsible for bringing the harvester's resonance frequency close to the

rotational driving frequency to achieve self-frequency tunability. The revolving tip tuning mass applies a variable centrifugal force on the tapered structure, modifying the beam's flexural rigidity by the resulting tensile stress. In contrast, the centrifugal force magnitude is increasing together with the rotational speed (driving frequency). So, if the increasing centrifugal force can shorten the harvester's effective length and increase the tensile stress, self-frequency-tuning can be achieved(Deng et al., 2020). Therefore, an efficient piezoelectric RVEH related to its resonant frequency can be designed by tracing the rotational driving frequency for a wide range.

5.2.1 Effect of taper parameter

The first principal resonance frequency of the RVEH against the input rotational frequency for a set of four various variation parameters (ϕ = 0(uniform cross-section), 5, 10, and 15) is depicted in Figure 5.10. The other parameters (t_p = 0.15 mm, r = 20 mm, l = 60 mm, b_0 = 50 mm, and t_h = 0.45 mm) are kept constant. An upsurge in the taper parameter decreases the principal natural frequency due to the decrease in the system's flexural rigidity. The frequency-matching point is the intersection point of the natural frequency curve and the desired frequency$\left(\omega_n = \omega_d\right)$ curve. When the two curves overlap in a definite band of frequency, the system attains self-tuning in that band. It can be observed that there is a single crossing point between the curves when the other system configurations remain unaltered. Thus, to attain self-tuning on a broader frequency band, we need different ϕ, which is complicated to realize in a practical scenario.

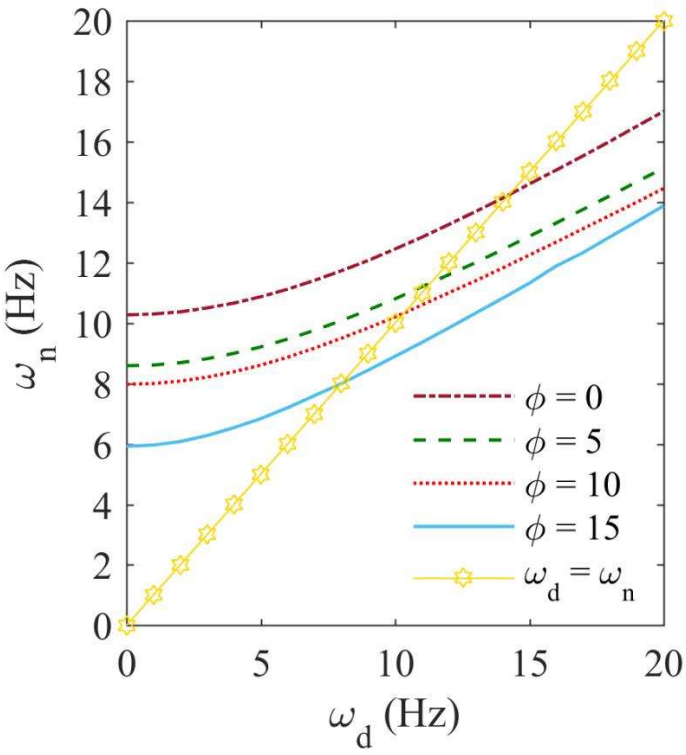

Figure 5.10 For various taper parameters with t_p = 0.15 mm, r = 20 mm, l = 60 mm, b_0 = 50 mm, and t_h = 0.45 mm; the calculated resonant frequency against the rotational driving frequency

The effect of the taper parameter variation on the output voltage of RVEH is also studied for the four taper parameter values. Figure 5.11 displays the harvester's voltage response curves for various taper parameters against rotational excitation frequencies. The harvested voltage is substantially reduced at higher rotational speeds as the taper parameter increases. However, the response is varied very slightly at lower speeds. This is because, at higher excitations, the nonlinearities associated with the geometry and piezoelectric materials become more evident. Although converging the width decreases the harvested voltage from the RVEH, the system's generated VPM should be used to evaluate the performance.

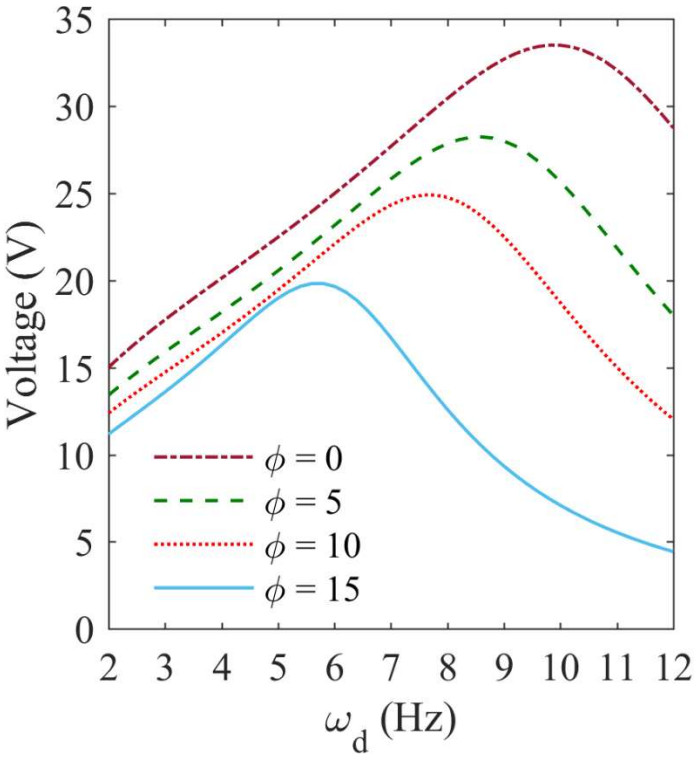

Figure 5.11 For various taper parameters with t_p = 0.15 mm, r = 20 mm, l = 60 mm, b_0 = 50 mm, and t_h = 0.45 mm; the output voltage response of the RVEH against the rotational driving frequency

5.2.2 Effect of the length of the piezoelectric coupled beam

Figure 5.12 displays that a decrease in the length of the piezoelectric-coupled beam increases the resonant frequency of the RVEH. This is caused by the rise in the rigidity of the beam. To attain frequency-matching on a broader band of driving frequencies, we need different l, which is possible in a practical situation(Deng et al., 2020). Again, it is very much evident in early reported research articles that all the vibration energy generators have the maximum efficiency when the driving frequency becomes equal or close to the system's natural frequency. Therefore, the resultant centrifugal force must essentially adjust the l to maintain the principal natural frequency of the RVEH same

as that of the driving frequency. This can be explained as, when the rotational frequency increases, the active length of the harvester should decrease, causing an increase in the natural frequency of the system. So, if the harvesting beam's active length can be shortened synchronously with an increase in rotational driving frequency, then self-tuning can be achieved.

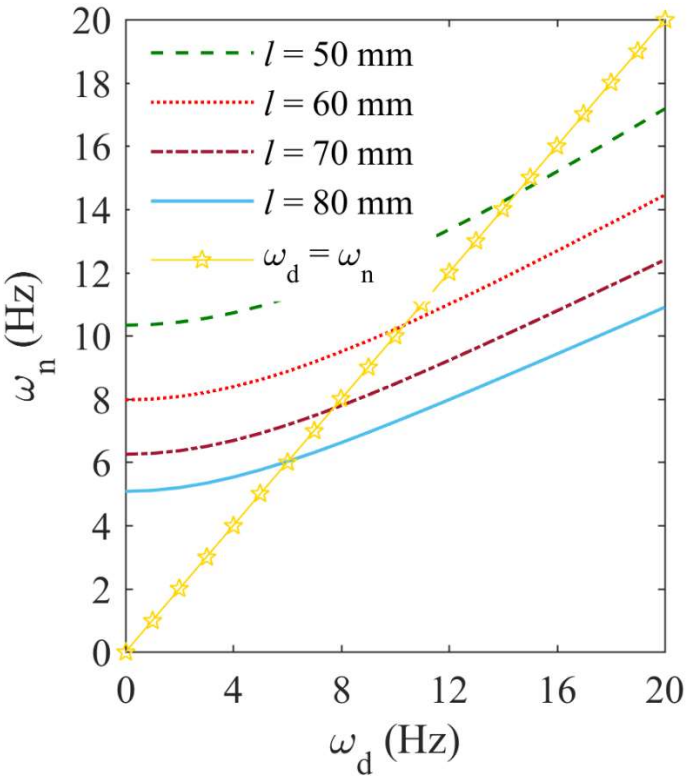

Figure 5.12 For various piezoelectric coupled beam lengths with t_p = 0.15 mm, r = 20 mm, ϕ = 10, b_0 = 50 mm, and t_h = 0.45 mm; the calculated resonant frequency against the rotational driving frequency

Figure 5.13 displays the harvester's open-circuit voltage curves for various piezoelectric beam lengths (l = 50, 60, 70, and 80 mm) and rotational excitation frequencies with t_p = 0.15 mm, r = 20 mm, ϕ = 10, b_0 = 50 mm, and t_h = 0.45 mm. The generated voltage decreased significantly with a decrease in the active length. This

is because of the availability of less piezoelectric surface area. Although raising the active length enhances the RVEH's generated voltage, the harvester's overall size imposes restrictions on the harvester's effective length. Therefore, a maximum beam length of 80 mm is considered in this analysis. Again, the VPM of the harvester is not essentially increased by increasing the harvesting beam length.

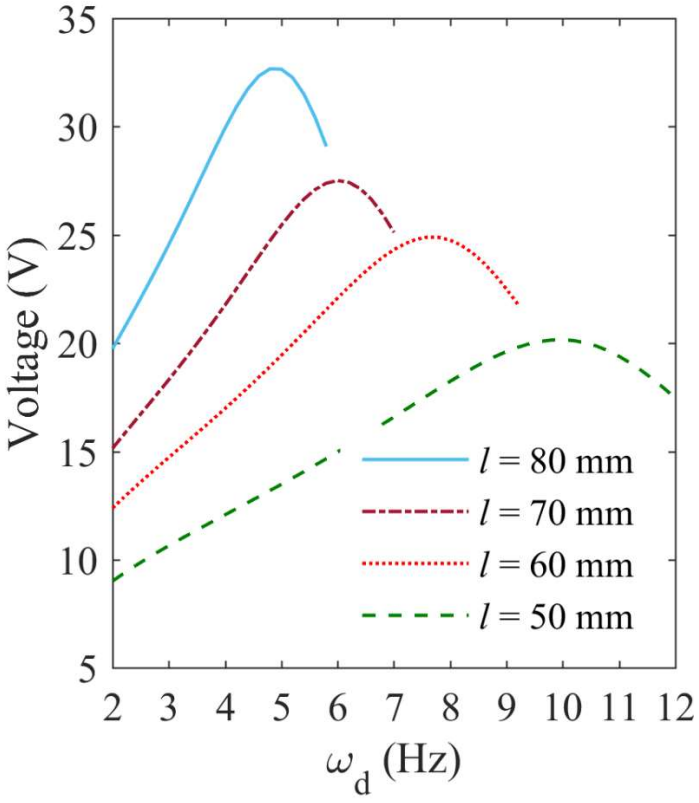

Figure 5.13 For various piezoelectric coupled beam lengths with t_p = 0.15 mm, r = 20 mm, ϕ = 10, b_0 = 50 mm, and t_h = 0.45 mm; the output voltage response of the RVEH against the rotational driving frequency

5.2.3 Effect of hub radius

The variation in the resonant frequencies for various rotating hub radiuses is shown in Figure 5.14. No zero-driving-frequency movement is observed by varying the hub

radius because of the centrifugal force's unavailability to produce extra tensile stress in the RVEH. In this case, the zero-driving frequency is considered as the resonant frequency of the RVEH at the rotational excitation frequency $\omega_d = 0$. Consequently, the zero-driving-frequency change indicates the resonant frequency change because of the variation in the hub radius, mass distribution, or geometrical shapes of the RVEH components at $\omega_d = 0$. When r is increased, the resonant frequency curve is modified to

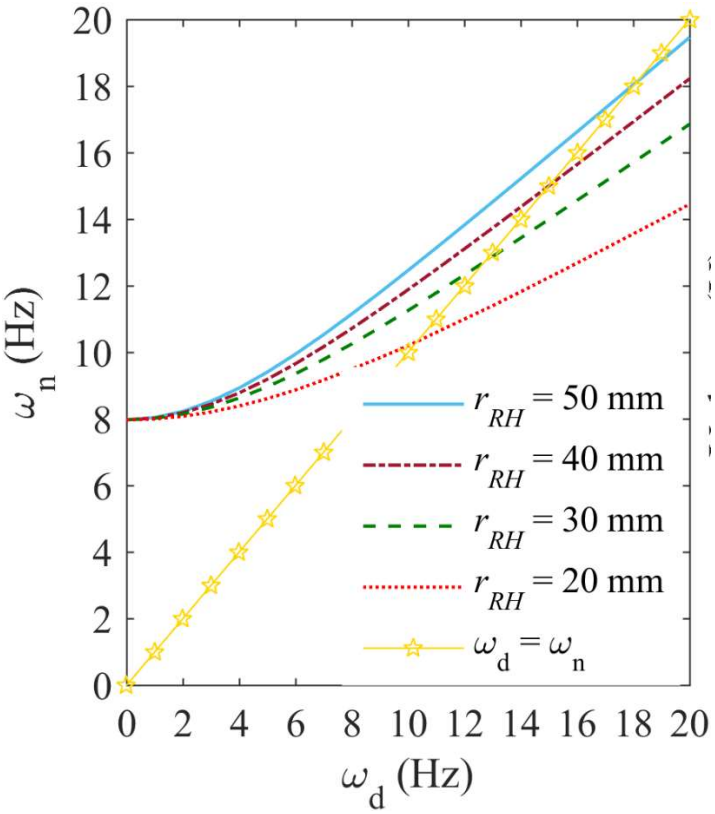

Figure 5.14 For various hub radiuses with t_p = 0.15 mm, l = 60 mm, ϕ = 10, b_0 = 50mm, and t_h = 0.45 mm; the calculated resonant frequency against the rotational driving frequency

be nearer to the curve of $\omega_n = \omega_d$. The increase in the hub radius causes growth in the centrifugal force to stiffen the piezoelectric-coupled structure. This is because the entire RVEH mass being positioned at a larger distance from the revolution axis. Therefore,

the performance affecting design parameters can be categorized into two kinds. The first category is operational in manipulating the fundamental frequency for power harvesting, where the zero-driving-frequency variation governs. The tip load mass, effective length, beam width, and thicknesses of the host and PZT patch are all included in this category. The second category (r) is operative for designing the self-matching frequency to be nearer to the rotational driving frequency for a broader frequency band, where the effect of centrifugal force dominates.

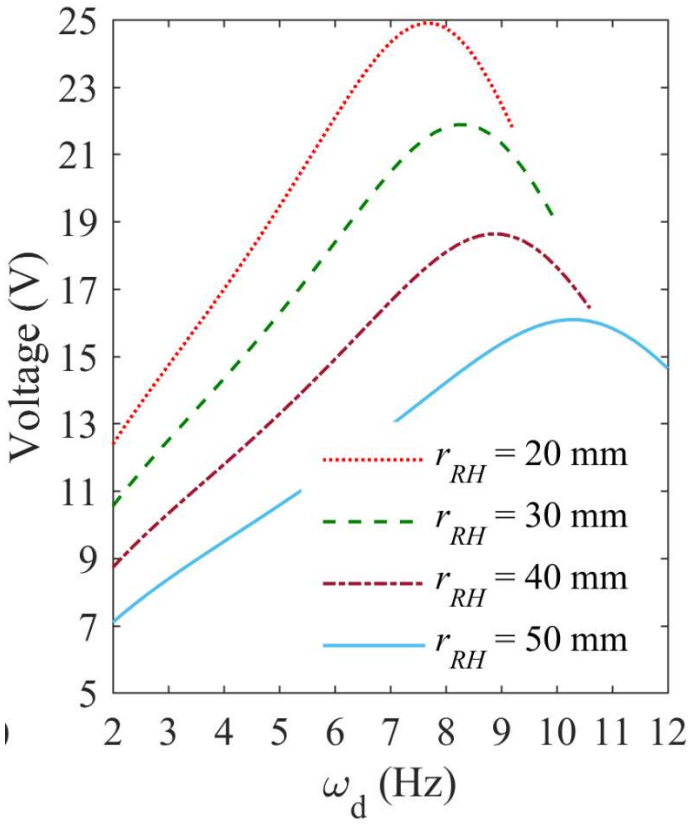

Figure 5.15 For various hub radiuses with t_p = 0.15 mm, l = 60 mm, ϕ = 10, b_0 = 50mm, and t_h = 0.45 mm; the generated voltage response of the RVEH against the rotational driving frequency

Figure 5.15 displays the open-circuit voltage for the RVEH with various r values (20, 30, 40, and 50 mm) and t_p = 0.15 mm, l = 60 mm, ϕ = 10, b_0 = 50 mm, and t_h = 0.45 mm. It can be observed that the frequency of the peak output voltage is moved rightward (higher frequencies) when the hub radius increases because of the increase in the resonance frequency values. In this case, the harvester's overall size also sets constraints on the hub radius's maximum value.

Varying the width does not essentially reduce the VPM of the RVEH as the volume and voltage decrease simultaneously. The VPM against the rotational frequency for different values of ϕ, l, and r are shown in Figure 5.16. The VPM is calculated as the peak of the voltage curve divided by the total volume of the harvester. The voltage curves' peaks in Figures 5.11, 5.13, and 5.15 are used for this purpose.

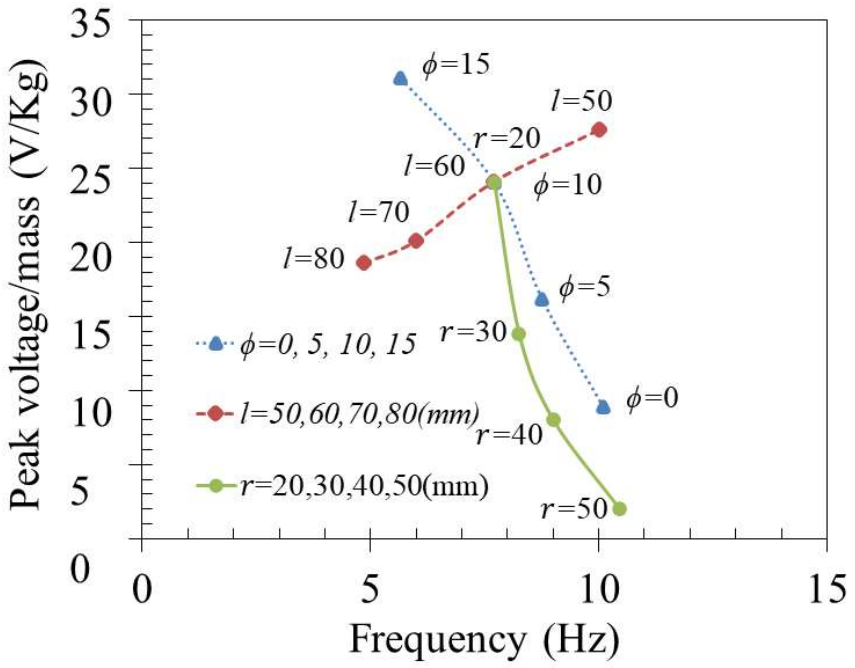

Figure 5.16 The VPM of the harvester against the driving rotational frequency for various values of ϕ, l, and r

The uniform beam has the lowest VPM, implying that tapering the width increases the power density from the RVEH. The VPM is severely suffered by the increase in hub radius as this effort decreases the output voltage and increases the total volume. The VPM of the harvester is also reduced with an increase in the harvester length. However, it is enriched with an increase in the taper parameter. Therefore, exponentially tapering the cross-section is advantageous.

Figures 5.17a – 5.17c show the simulated resonance frequency (SRF) of the peak OC output voltage and calculated matched frequency (CMF) of the RVEH as a function of r, l and ϕ, respectively. The SRF is the driving frequency at which the peak of the voltage curves appears in ANSYS simulation. The CMF is the intersection point of the resonant frequency curve and the $\omega_n = \omega_d$ curve. The simulated frequency values of the peak output voltage are a little less than the matching counterparts acquired from the analysis. The eccentricity may be caused by a discrepancy between the simulation and real material parameters and damping ratio values.

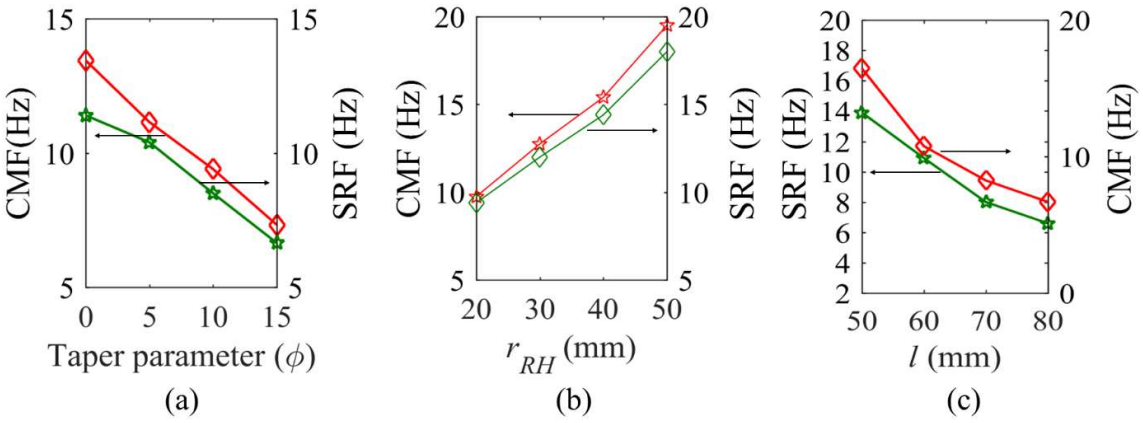

Figure 5.17 Comparison of the calculated matching frequencies of the RVEH and the simulated frequencies of the peak output voltage against (a) ϕ (b) r (c) l

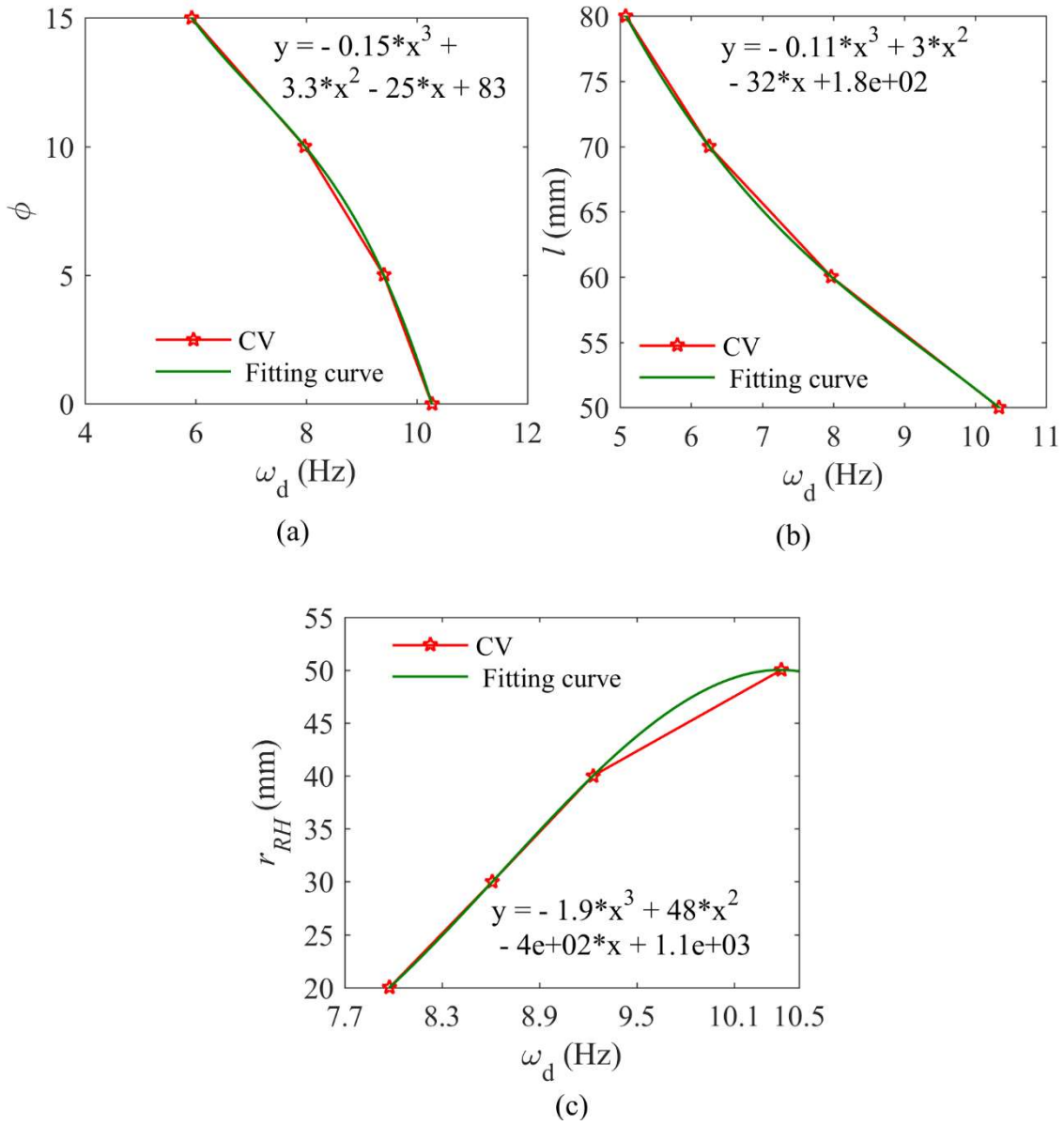

Figure 5.18 The (a) exponential taper parameter, (b) effective length of the PZT-coupled beam, and (c) hub radius, with driving frequency under the achieved frequency matching

The calculated matching frequency points in Figures 5.10, 5.12, and 5.14 are connected to obtain the calculated frequency value (CV) curves, displayed in Figures 5.18a – 5.18c, respectively. The fitting curves for the CV curves are also obtained. The taper parameter, effective beam length, and the hub radius, essential to accomplish frequency-

matching at any particular driving frequency, can be obtained from the respective fitting curves. The curve's precision is checked by selecting two arbitrary points for comparison, and higher accuracy is observed.

Figure 5.19 displays the generated power of the RVEH versus the resistive load R working at the resonant frequencies. Here the resonant frequency implies the measured frequencies having the peak output voltage in Figures 5.11, 5.13, and 5.15. The plot is shown for a system having $t_p = 0.15$ mm, $l = 60$ mm, $\phi = 10$, $b_0 = 50$ mm, $t_h = 0.45$ mm and hub radiuses equal to 10, 20, 30, and 40 mm. The case of $r = 20$ mm gives a maximum output power of 2.71 mW with a power density of 5.27 μW mm^{-3} and PAF of 3.14 across the optimum load resistance of 300 kΩ.

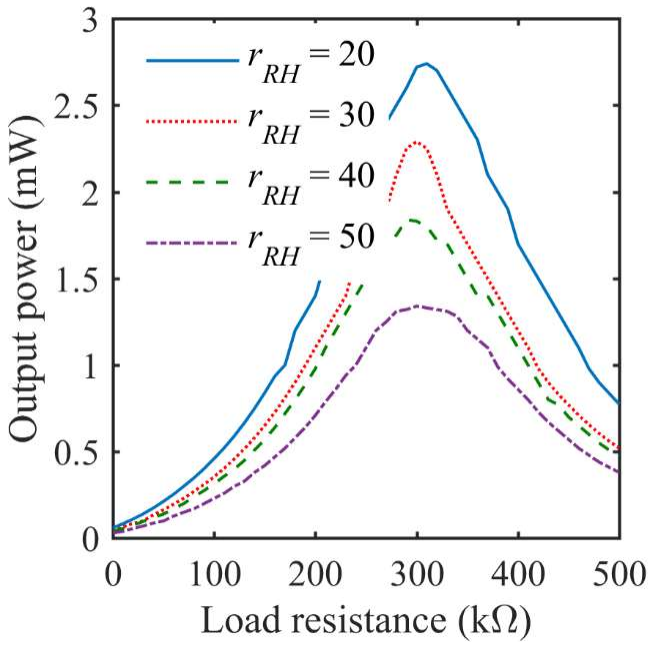

Figure 5.19 Comparison of the generated power of the RVEH versus resistance R, functioning at its measured resonant frequencies related with hub radiuses equal to 20, 30, 40, and 50 mm with $t_p = 0.15$ mm, $l = 60$ mm, $\phi = 10$, $b_0 = 50$ mm, and $t_h = 0.45$ mm

An increase in the hub radius decreases the generated output power because of the same factors, which decreases the voltage responses. It can be noticed that the optimum resistances occur at around 300 kΩ for all the cases. An increase in the r (or alternatively, increasing the generated centrifugal force) marginally reduces the optimum load resistance value. The centrifugal force generated from rotation increases the harvester's effective stiffness and modifies its other properties to shift the optimum resistance value. In general, the electromechanical coupling coefficient, the damping ratio, and the harvester's operating frequency affect the optimum resistance for generating maximum power.

5.3 Summary

The findings of this chapter can be summarized as follows;

1. An increase in the taper parameter decreases the generated voltage and vice versa for the VPM
2. Increasing the thickness ratio increases both the output voltage and the VPM.
3. An increase in the length of the piezoelectric-coupled beam increases the generated voltage and the VPM
4. The increase in the overall radius of rotation, diminishing the OC voltage responses.
5. In addition, the harvester's overall size set constraints on the maximum value of the radius of rotation and the length
6. The proposed harvester's responses presented in this chapter can be implemented in combination with additional efficiency-enhancing techniques to improve the power output. For example, attaching another PZT patch to the

lower side of the host beam and making provisions for harvesting from higher vibration modes can be used. However, geometric nonlinearities are inevitable with bimorph harvesters and at a higher level of excitations. Frequency self-tuning techniques like changing the effective length and mass centre position can be implemented with the proposed model to achieve a broadband operation.